



UNIVERSITY OF LEEDS

This is a repository copy of *Steam reforming of different biomass tar model compounds over Ni/Al<sub>2</sub>O<sub>3</sub> catalysts*.

White Rose Research Online URL for this paper:  
<http://eprints.whiterose.ac.uk/111286/>

Version: Accepted Version

---

**Article:**

Artetxe, M, Alvarez, J, Nahil, MA et al. (2 more authors) (2017) Steam reforming of different biomass tar model compounds over Ni/Al<sub>2</sub>O<sub>3</sub> catalysts. *Energy Conversion and Management*, 136. pp. 119-126. ISSN 0196-8904

<https://doi.org/10.1016/j.enconman.2016.12.092>

---

© 2017 Elsevier Ltd. This manuscript version is made available under the CC-BY-NC-ND 4.0 license <http://creativecommons.org/licenses/by-nc-nd/4.0/>

**Reuse**

Unless indicated otherwise, fulltext items are protected by copyright with all rights reserved. The copyright exception in section 29 of the Copyright, Designs and Patents Act 1988 allows the making of a single copy solely for the purpose of non-commercial research or private study within the limits of fair dealing. The publisher or other rights-holder may allow further reproduction and re-use of this version - refer to the White Rose Research Online record for this item. Where records identify the publisher as the copyright holder, users can verify any specific terms of use on the publisher's website.

**Takedown**

If you consider content in White Rose Research Online to be in breach of UK law, please notify us by emailing [eprints@whiterose.ac.uk](mailto:eprints@whiterose.ac.uk) including the URL of the record and the reason for the withdrawal request.



[eprints@whiterose.ac.uk](mailto:eprints@whiterose.ac.uk)  
<https://eprints.whiterose.ac.uk/>

1     **Steam reforming of different biomass tar model compounds**  
2                                   **over Ni/Al<sub>2</sub>O<sub>3</sub> catalysts**

3     Maite Artetxe<sup>b\*</sup>, Jon Alvarez<sup>b</sup>, Mohamad A. Nihil<sup>a</sup>, Martin Olazar<sup>b</sup>, Paul T. Williams<sup>a</sup>

4             <sup>a</sup> School of Chemical & Process Engineering, University of Leeds, Leeds LS2 9JT,  
5                                   United Kingdom

6             <sup>b</sup> Department of Chemical Engineering, University of the Basque Country, P.O. Box  
7                                   644 - E48080, Bilbao, Spain

8

9                                   [maite.artetxe@ehu.eus](mailto:maite.artetxe@ehu.eus)

10                                Tel.: +34 946 015 414

11                                Fax: +34 946 013 500

12

13 **Abstract**

14 This work focuses on the removal of the tar derived from biomass gasification by  
15 catalytic steam reforming on Ni/Al<sub>2</sub>O<sub>3</sub> catalysts. Different tar model compounds  
16 (phenol, toluene, methyl naphthalene, indene, anisole and furfural) were individually  
17 steam reformed (after dissolving each one in methanol), as well as a mixture of all of  
18 them, at 700 °C under a steam/carbon (S/C) ratio of 3 and 60 min on stream. The  
19 highest conversions and H<sub>2</sub> potential were attained for anisole and furfural, while  
20 methyl naphthalene presented the lowest reactivity. Nevertheless, the higher reactivity  
21 of oxygenates compared to aromatic hydrocarbons promoted carbon deposition on the  
22 catalyst (in the 1.5-2.8 wt. % range). When the concentration of methanol is decreased  
23 in the feedstock and that of toluene or anisole is increased, the selectivity to CO is  
24 favoured in the gaseous products, thus increasing coke deposition on the catalyst and  
25 decreasing catalyst activity for the steam reforming reaction. Moreover, an increase in  
26 Ni loading in the catalyst from 5 to 20 % enhances carbon conversion and H<sub>2</sub> formation  
27 in the steam reforming of a mixture of all the model compounds studied, but these  
28 values decrease for a Ni content of 40 %. Coke formation also increased by increasing  
29 Ni loading, attaining its maximum value for 40 % Ni (6.5 wt. %).

30 **Keywords:** Ni/Al<sub>2</sub>O<sub>3</sub> catalyst, biomass gasification, tar model compound, steam  
31 reforming

32

33

## 34 **1. Introduction**

35 Biomass gasification is regarded as a promising technology in the development of a  
36 worldwide sustainable energy system. The major product in this thermochemical  
37 process is a combustible gas (also called syngas) that may be used for power generation  
38 (gas turbines, fuel cells or engines) or as feedstock for the synthesis of liquid fuels via  
39 Fischer-Tropsch and various chemical products [1]. However, this syngas also contains  
40 some impurities, such as fine particles, organic tars, NO<sub>x</sub> and SO<sub>2</sub>, which need to be  
41 removed before its application [2].

42 In particular, tars are the main contaminants in the gas produced and their content  
43 ranges from 5 to 100 g/Nm<sup>3</sup>, depending on the type of gasifier. However, their  
44 maximum allowable content is 5 mg/Nm<sup>3</sup> in gas turbines and 100 mg/Nm<sup>3</sup> in internal  
45 combustion engines [3, 4]. Tars are a complex mixture of aromatic and oxygenated  
46 hydrocarbons that may cause several operational problems, such as condensation and  
47 subsequent plugging of downstream equipment, clogging filters, metal corrosion,  
48 polymerization into more complex structures and coke deposition on the catalyst [5, 6].  
49 Hence, tar elimination is essential in order to implement any technology for syngas  
50 exploitation.

51 Amongst the different strategies to remove tars from the gas [4], catalytic steam  
52 reforming seems to be a promising alternative from an economic and technical point of  
53 view, given that a high degree of gas purity can be attained and, at the same time, the  
54 product gas heating value is increased [6, 7]. This process involves the oxidation of the  
55 tar components using steam to produce a useful gas (mainly H<sub>2</sub> and CO) and the  
56 presence of a catalyst allows a more effective tar removal at lower temperatures than  
57 non-catalytic tar conversion. Ni-based catalysts have been widely applied in the steam  
58 reforming of biomass tars due to their low cost, high activity for C-C and O-H bond

59 rupture and better performance in terms of H<sub>2</sub> production [8-13]. The high activity of  
60 Ni/Al<sub>2</sub>O<sub>3</sub> catalysts is attributed to the high metal surface area and high thermal stability  
61 [14]. However, these types of catalysts are usually deactivated by coke deposition on  
62 the active sites and sintering on the catalyst surface [15]. Several strategies have been  
63 proposed in order to minimize catalyst deactivation, such as process configuration (one  
64 or two stages) [16], optimization of operating conditions (temperature, S/C ratio and  
65 space time) [17, 18] and catalyst improvement (with different Ni loadings, additives or  
66 supports) [19].

67 Although there are papers in the literature dealing with the steam reforming of real  
68 biomass tars [19-22], the complexity of tar composition makes it difficult to ascertain  
69 both the reaction mechanism and the main species responsible for catalyst deactivation  
70 by coke deposition. Therefore, most of the literature focuses on the conversion of  
71 individual model molecules, usually toluene, benzene, phenol or naphthalene on  
72 supported metal catalysts [5, 7, 9, 23, 24], but only few papers compare their reactivities  
73 and trends towards coke formation [3, 25-27]. Furthermore, since tar is a mixture of  
74 organic compounds with different structure and molecular weight affecting product  
75 distribution and coke nature, a deeper understanding on the behaviour of tar main  
76 components and their mixture is required in the steam reforming process.

77 Based on this background, this paper focuses on a systematic and detailed comparison  
78 of a series of model compounds and their mixture in the catalytic steam reforming  
79 process in terms of hydrogen production and catalyst deactivation. The components  
80 selected are representative of the major chemical families contained in the tar derived  
81 from biomass gasification, i.e., phenol, toluene, methyl naphthalene, indene, anisole and  
82 furfural. In addition, as the steam reforming reactions were carried out over a typical  
83 reforming catalyst (Ni/Al<sub>2</sub>O<sub>3</sub>), the influence of Ni loading was also investigated by

84 feeding a mixture of all the model compounds studied. The operating conditions were  
85 based on the results of a previous work about phenol steam reforming, in which  
86 temperature, space time and reaction time were optimized in order to maximize  
87 conversion and minimize coke deposition [18]. The study is conducted not only with the  
88 aim of eliminating biomass gasification tars and converting them into higher value  
89 added products, such as hydrogen, but also with the aim of contributing to a better  
90 understanding of the steam reforming behavior of the most representative tar  
91 compounds on a low-cost and high activity catalyst like Ni/Al<sub>2</sub>O<sub>3</sub>, by considering the  
92 influence each compound has on the catalyst deactivation by coke deposition. This issue  
93 is essential in order to find the species responsible for the different reactivity and coke  
94 formation, with the latter hindering the good performance of the catalysts in the tar  
95 reforming process

## 96 **2. Experimental**

### 97 2.1. Model compounds

98 Six compounds were selected: phenol, toluene, methyl naphthalene, indene, anisole and  
99 furfural. These compounds cover a wide range of one- and two-ring aromatic  
100 hydrocarbons and oxygen containing compounds present in the tars derived from  
101 biomass gasification. In addition, given that some model compounds were solid at room  
102 temperature, methanol was used as solvent in all the experiments and, in order to assess  
103 its contribution to the final product stream, it was previously steam reformed alone.

### 104 2.2. Catalyst preparation

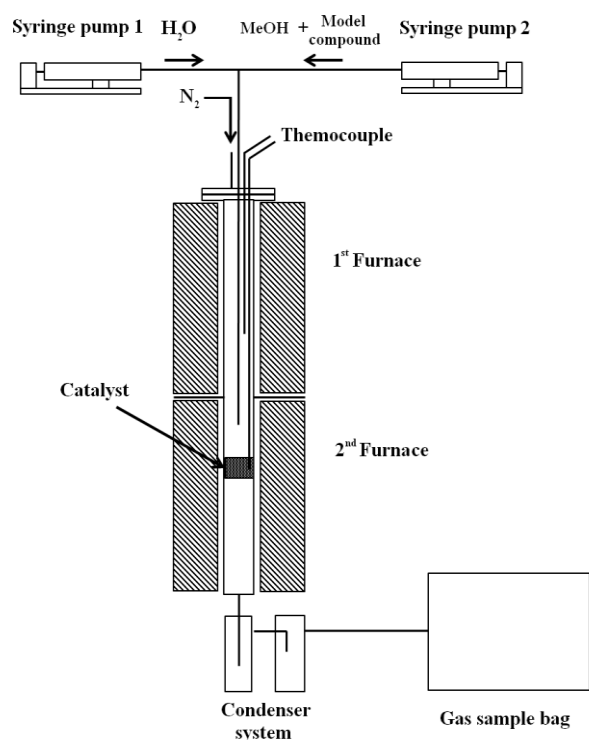
105 The Ni/Al<sub>2</sub>O<sub>3</sub> catalysts were prepared by the impregnation method, in which the  $\gamma$ -  
106 Al<sub>2</sub>O<sub>3</sub> (96% Alfa Aesar) support was impregnated with an aqueous solution of  
107 Ni(NO<sub>3</sub>)<sub>2</sub>·6H<sub>2</sub>O (Sigma-Aldrich). The resulting solution was continuously stirred for 30

108 min at 100 °C followed by drying at 105 °C overnight, and it was then calcined  
109 following a heating rate of 20 °C min<sup>-1</sup> in an air atmosphere at 750 °C for 3 h. Finally,  
110 the catalysts prepared were ground and sieved to a size between 0.18 and 0.24 mm and  
111 reduced in-situ by the process gases (H<sub>2</sub> and CO) generated during the reaction, as was  
112 reported in previous papers, [15, 18]. The catalysts were formulated with Ni loadings of  
113 5, 10, 20 and 40 wt. %, respectively.

### 114 2.3. Experimental equipment and procedure

115 The steam reforming experiments of the model compounds and their mixture on  
116 Ni/Al<sub>2</sub>O<sub>3</sub> catalysts were performed in a two-stage stainless steel tube reactor (both 16  
117 cm in length and 2.2 cm in internal diameter), placed within two independently heated  
118 electric furnaces, as shown in Figure 1. The water and the blend of the model  
119 compound with methanol were fed into the first reactor by means of syringes 1 and 2,  
120 respectively. This reactor was maintained at 250 °C in order to ensure a complete  
121 vaporization of the feedstock before entering the next reactor containing the catalyst. In  
122 addition, a nitrogen flow rate of 80 ml min<sup>-1</sup> was introduced to sweep the volatiles  
123 formed in the reactor. The model compounds and their mixture were steam reformed at  
124 750 °C for 60 min in the second reactor, in which 1.5 g of Ni/Al<sub>2</sub>O<sub>3</sub> catalyst were  
125 previously placed. The products generated in the steam reforming process were cooled  
126 by passing through two condensers filled with dry ice, which gathered the liquid water  
127 and the unconverted model compounds. All the non-condensable gases were collected  
128 using a 10 L Teldar<sup>TM</sup> gas sample bag. After finishing each experiment, the gases were  
129 collected for another 20 min to ensure the reaction was complete. The amount of  
130 unconverted reactant was calculated by weighing both syringes and the condensers  
131 before and after the experiments. The gases collected in the gas sample bag were  
132 analysed off-line by gas chromatography following the same methodology reported in

133 previous papers [15, 18]. All the experiments were repeated at least twice to ensure  
134 reproducibility of the results.



135

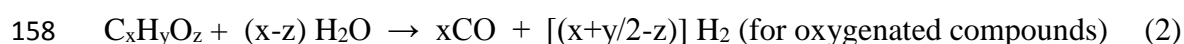
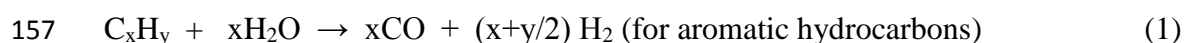
136

**Figure 1**

137 The catalyst loaded with 10 wt% Ni was used to investigate the reactivity of the  
138 different tar compounds in the steam reforming process and their influence on the  
139 product distribution and catalyst deactivation. In these experiments, the atomic ratio for  
140 model compound carbon atoms / solvent carbon atoms ( $C_{cc}/C_s$ ) was kept always at 1. In  
141 addition, in order to investigate the effect of  $C_{cc}/C_s$  ratio in the steam reforming  
142 reaction, experiments were performed by feeding toluene and anisole with a  $C_{cc}/C_s$   
143 ratio of 2. Moreover, the influence of Ni loading (5, 10, 20 and 40 wt%) on the  
144 conversion of a mixture of all the tar model compounds was also analyzed, by keeping  
145 in this case the  $C_s/C_{cc}$  ratio at 1. All the experiments were carried out at a S/C ratio of 3,  
146 which meant that water flow rate was always 6.64 ml h<sup>-1</sup>. However, the flow rate for

147 each model compound was different: 4.97 ml min<sup>-1</sup> for methanol, 3.41 ml min<sup>-1</sup> for  
148 toluene, 2.48 ml min<sup>-1</sup> for phenol, 3.28 ml min<sup>-1</sup> for indene, 3.44 ml min<sup>-1</sup> for anisole,  
149 3.26 ml min<sup>-1</sup> for methylnaphthalene, 3.5 ml min<sup>-1</sup> for furfural and 3.1 ml min<sup>-1</sup> for the  
150 mixture of all the model compounds used in the experiments involving different Ni  
151 loadings. It should be noted that these flow rates are based on the mixture of methanol  
152 and the model compound(s).

153 Many parallel reactions may occur during the catalytic steam reforming process and  
154 product distribution is the result of their competition [28], with the most important  
155 being those of steam reforming (Eq. 1 and 2) and water gas shift (WGS) (Eq. 3), as  
156 shown below [27]:



160 In order to quantify the products of the reforming process, conversion and product  
161 yields have been taken as reaction indices. The carbon conversion of the model  
162 compounds was defined as the moles of carbon in the gaseous product stream divided  
163 by the moles of carbon in the feed. Furthermore, the moles of CO, CO<sub>2</sub> and C<sub>1</sub>- C<sub>4</sub>  
164 hydrocarbons formed during the reaction have been determined from GC analyses,  
165 which allowed calculating the total amount of carbon moles in the gas. The moles of  
166 carbon in the feed were calculated based on the total amount of model compound or  
167 mixture introduced into the reactor, i.e, weighing the syringe before and after the  
168 experiment. The product yields were calculated as the ratio between the grams of each  
169 product (H<sub>2</sub>, CO, CO<sub>2</sub> and CH<sub>4</sub>) in the gaseous stream and the grams of the model  
170 compound in the feed.

171 C conversion (%) =  $\frac{\text{moles of carbon in the product gas}}{\text{moles of carbon in the feed}} \times 100$  (4)

172 Yield (%) =  $\frac{\text{g of the compound in the product gas}}{\text{g of the model compound in the feed}} \times 100$  (5)

173 Moreover, H<sub>2</sub> potential was also determined as the ratio between the concentration of H<sub>2</sub>  
174 in the effluent gas and the maximum allowed by stoichiometry:

175 H<sub>2</sub> potential =  $\frac{\text{moles of H}_2 \text{ in the product gas}}{\text{maximum moles of H}_2 \text{ allowed by stoichiometry}} \times 100$  (6)

176 The maximum number of H<sub>2</sub> moles allowed by stoichiometry was calculated by  
177 considering reforming and WGS reactions i.e. reactions 1 and 3 for aromatic  
178 hydrocarbons and reactions 2 and 3 for oxygenated compounds. Thus, H<sub>2</sub> potential is  
179 defined based on the maximum number of H<sub>2</sub> moles obtained when model compounds  
180 are fully reformed to CO<sub>2</sub> and H<sub>2</sub>.

#### 181 2.4. Characterization of the used catalyst

182 The amount and nature of the coke deposited on the catalyst were determined by  
183 temperature-programmed oxidation (TPO) using a thermogravimetric analyzer  
184 (Shimadzu TGA-50). The catalyst was fully recovered after the reaction and around 20  
185 mg were used for determining the coke content by TPO. The sample was heated in an  
186 atmosphere of air at 15 °C min<sup>-1</sup> to a final temperature of 800 °C and maintained at this  
187 temperature for 10 min. In addition, a Hitachi SU8230 high-resolution scanning electron  
188 microscope (SEM) was used to analyze the surface morphology of the used catalyst and  
189 the nature of the coke deposited on it.

190

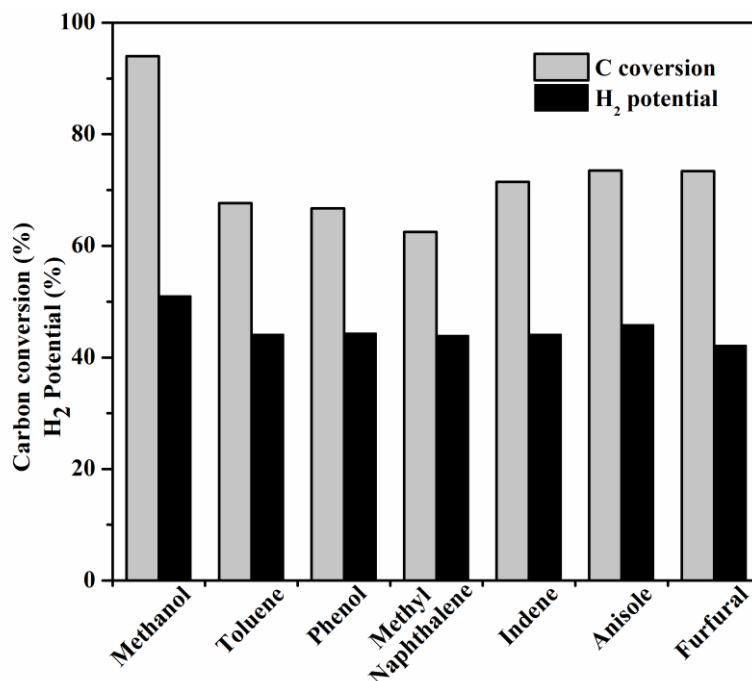
### 191 3. Results and discussion

### 192 3.1. Steam reforming of model compounds

193 The catalytic steam reforming of different tar model compounds was carried out on a  
194 Ni/Al<sub>2</sub>O<sub>3</sub> catalyst and Figure 2 shows a comparison of their conversions and H<sub>2</sub>  
195 potential at 750 °C catalyst temperature and after 60 min on stream. The mechanism of  
196 catalytic steam reforming involves the absorption of model molecules and water vapour  
197 on the catalyst surface, where they react with CO, CO<sub>2</sub> and H<sub>2</sub>, as observed in reactions  
198 (1-3). S/C ratio of 3 is an adequate value for tar conversion and product gas  
199 composition, given that although a high water concentration will promote the WGS  
200 reaction, most active sites on the catalyst surface would be occupied by H<sub>2</sub>O molecules  
201 at very high S/C ratios, thereby resulting in a lower adsorption capacity and lower tar  
202 conversion. Given that all the compounds were dissolved in methanol, Figure 2 also  
203 provides information on the conversion and H<sub>2</sub> potential for this solvent in the steam  
204 reforming process. As observed, the conversion of all the model compounds was in the  
205 63-75 % range, which is lower than that of methanol (94 %). The most reactive  
206 compounds were furfural and anisole, followed by indene and toluene, with the most  
207 refractory one being methyl naphthalene. Also, the H<sub>2</sub> potential for all the model  
208 compounds studied was very similar, with values between 42 and 45 %.

209 These results obtained in this work suggest that there are significant differences in the  
210 steam reforming mechanism of hydrocarbons and oxygenates. Thus, larger cyclic  
211 hydrocarbons with higher molecular weight are less reactive, whereas those containing  
212 oxygen-carbon bonds are more easily reformed [29]. In addition, these oxygenates are  
213 more thermally unstable, thereby undergoing homogeneous (gas-phase) thermal  
214 decomposition, as well as cracking reactions on the acid sites on the catalyst support,  
215 competing with the steam reforming to H<sub>2</sub> [30]. It is noteworthy that phenol underwent  
216 the lowest conversion among the oxygenated compounds. According to Wang et al.

217 [17], the formation of more stable intermediates during the reforming of phenol  
218 increases the difficulty in decomposing this compound on the Ni surface compared to  
219 the other oxygenates, such as furfural or hydroxyacetone.



220

221

**Figure 2**

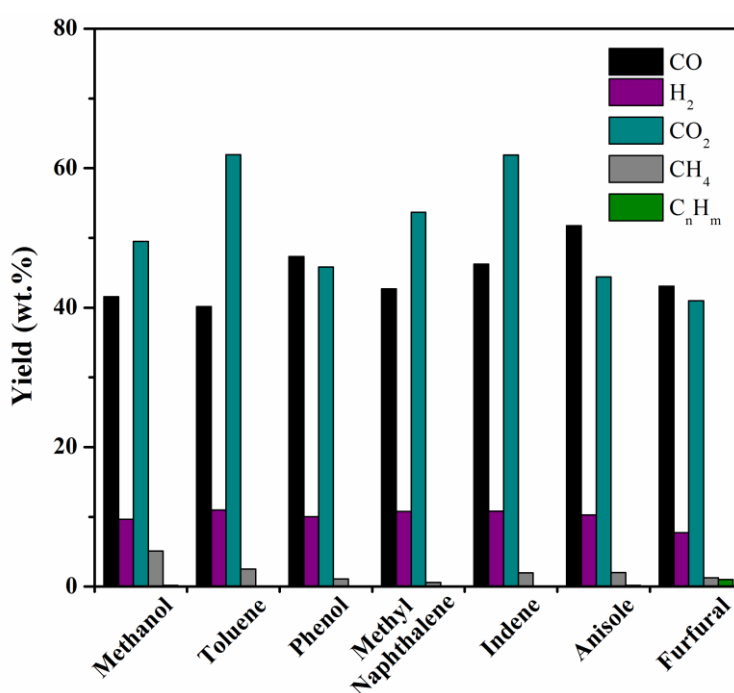
222 Similar results have been reported in the literature for the steam reforming of model  
223 compounds, i.e., naphthalene is reported to be less reactive than other tar compound  
224 models, such as toluene, benzene, pyrene or anthracene [3, 19, 26, 28]. In addition, Hu  
225 and Lu [31] and Davda et al [32] concluded that oxygen containing hydrocarbons, such  
226 as glucose (with a C/O ratio of 1), may be completely and faster converted than  
227 hydrocarbons with a similar number of carbon atoms, given that the steam reforming of  
228 these compounds to CO and H<sub>2</sub> is thermodynamically favoured at low temperatures.

229 The yields of the gaseous compounds obtained in the steam reforming of the model  
230 compounds are displayed in Figure 3. As observed, the major products are CO and CO<sub>2</sub>  
231 followed by H<sub>2</sub>, which makes clear that the main reaction taking place on the Ni/Al<sub>2</sub>O<sub>3</sub>  
232 catalyst is that of steam reforming (Eq. 1 and 2) followed by WGS (Eq. 3). The

233 common reaction scheme proposed in the literature [19] for the steam reforming process  
234 consists of C-H or C-C bond cleavage onto the metal surface to form carbon (C\*) and  
235 H<sub>2</sub>. Then, the C\* species react with the hydroxyl groups derived from the dissociation  
236 of H<sub>2</sub>O (OH\*) on the support to form CO, which will further react with the remaining  
237 H<sub>2</sub>O to give more H<sub>2</sub> and CO<sub>2</sub> [9]. The highest yields of CO<sub>2</sub> are obtained from  
238 aromatic hydrocarbons, i.e., toluene (62 wt. %), indene (61 wt. %) and  
239 methylnaphthalene (53 wt. %), whereas CO formation is more favoured for oxygenated  
240 hydrocarbons like anisole (52 wt. %) and phenol (47 wt. %). The parallel formation of  
241 CO intermediate from the direct decomposition of each compound due to presence of  
242 oxygen atoms in the molecule would promote the production of CO in the gaseous  
243 stream [12]. Furthermore, the CO/CO<sub>2</sub> ratio depends on the WGS equilibrium reaction  
244 and, as observed, the higher amount of CO in the gaseous stream derived from phenol,  
245 anisole and furfural and the lower content of CO<sub>2</sub> and H<sub>2</sub> are evidences that these  
246 oxygenated compounds enhance the reverse WGS reaction by displacing the  
247 thermodynamic equilibrium to the endothermic route [6, 33]. In this context, two  
248 possible mechanisms for phenol decomposition on nickel surface were explained in a  
249 previous paper [18], in which it was concluded that both mechanisms lead mainly to the  
250 formation of CO and H<sub>2</sub>. Other authors have also highlighted that the carbon deposited  
251 on the catalyst may further react with steam to generate additional CO and so contribute  
252 to keeping catalyst activity [5].

253 In addition, the content of CH<sub>4</sub> was very low and that of C<sub>2</sub>-C<sub>4</sub> hydrocarbons almost  
254 negligible in all the experiments. These results confirm that these model compounds,  
255 especially those with aromatic rings, are quite refractory to cracking reactions (more  
256 refractory as the number of rings is increased). In fact, methyl naphthalene with 2  
257 aromatic rings (more than any other model compound studied) leads to the lowest CH<sub>4</sub>

258 yield (0.6 wt. %). It should be noted that the reforming of toluene and anisole leads to a  
259 slightly higher concentrations of CH<sub>4</sub> than the other model compounds due to the  
260 dealkylation of the methyl group in its structure [28]. The CH<sub>4</sub> formed may also be  
261 derived from the decomposition of the model compound itself or from CO through the  
262 methanation reaction [3, 12, 23]. However, these reactions are almost irrelevant because  
263 the CH<sub>4</sub> content in the product gases was less than 4 %.



264

265

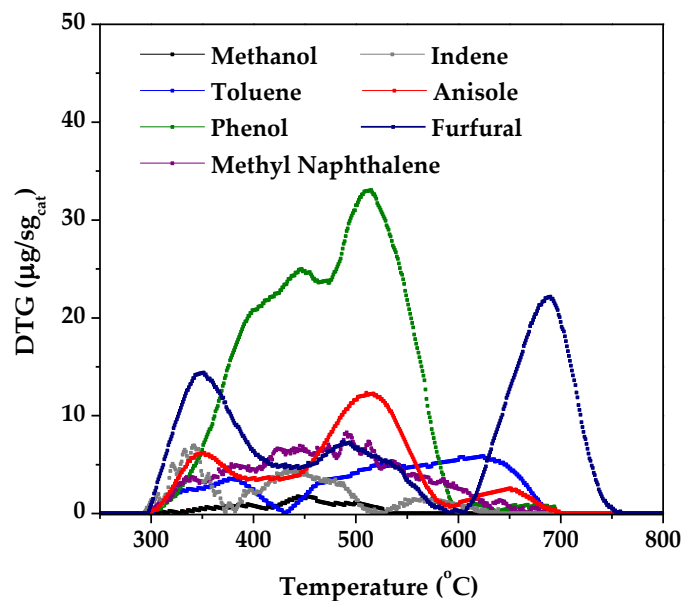
**Figure 3**

266 The nature and amount of the coke deposited on the catalyst in the steam reforming of  
267 different model compounds were determined by temperature programmed oxidation  
268 (DTG-TPO) curves (Figure 4). This coke blocks the pores and poisons the active sites,  
269 which leads to a loss of activity in the catalyst, and consequently hydrogen production is  
270 reduced. However, the addition of steam reduces coke deposition on the catalyst, given  
271 that the carbon generated may further react with the water in the medium. Thus, the low  
272 amount of coke formed on the used catalysts is noteworthy (lower than 2.8 wt. % in all  
273 cases), which is evidence that the operating conditions selected (1.5 g of catalyst, 750

274 °C and S/C=3) limit coke development. The content of coke deposited was higher in  
275 those experiments performed with oxygenated compounds, being 2.8, 2.7 and 1.5 wt. %  
276 for phenol, furfural and anisole, respectively. On the contrary, the steam reforming of  
277 aromatic hydrocarbons resulted in lower coke deposition (in the 0.5-0.8 wt. % range).  
278 The tar compounds studied tend to undergo thermal decomposition and/or cracking  
279 reactions together with the Boudouard reaction ( $2\text{CO} \leftrightarrow \text{CO}_2 + \text{C}_{\text{solid}}$ ), which compete  
280 with the steam reforming reaction. Therefore, the higher reactivity of oxygenated  
281 compounds compared to hydrocarbons would enhance these unwanted reactions, thus  
282 favouring coke formation [29]. The carbon formed via decomposition usually tends to  
283 accumulate at the initial section of the catalytic bed due to the high partial pressure of  
284 the reactants, whereas that produced via CO disproportionation would be accumulated at  
285 the final section due to the high CO partial pressure at this position in the catalytic bed.  
286 Other papers have also reported the higher coke deposition from oxygen containing  
287 model compounds. For example, Koike et al. [9] determined that the carbon deposition  
288 originated from the steam reforming of phenol was higher than that from toluene and  
289 benzene. Remón et al. [34] concluded that furfural had the highest influence in terms of  
290 carbon deposition on the catalyst in the reforming of the aqueous fraction of bio-oil on a  
291 Ni-Co/Al-Mg catalyst. Trane-Restrup and Jensen [27] also found a higher coke  
292 deposition rate on Ni/CeO<sub>2</sub>-K/MgAl<sub>2</sub>O<sub>4</sub> catalyst for furfural and guaiacol than for 2-  
293 methylfuran and ethanol, which is explained by their lower molecular weight.

294 As observed in Figure 4, the number of peaks observed in the TPO profiles and the  
295 temperatures corresponding to these peaks (between 250 and 700 °C) provide  
296 information about the heterogeneity of the coke (more heterogeneous coke as the  
297 number of peaks is higher). The results in the literature about coke deposition on  
298 Ni/Al<sub>2</sub>O<sub>3</sub> reforming catalyst [16, 18, 35] allow establishing the hypothesis that coke is

299 heterogeneous, with mainly three preferential oxidation peaks: i) around 350-400 °C  
300 oxidation temperature, which can be attributed to the amorphous external coke (also  
301 known as encapsulating coke) deposited over Ni particles, which is easily accessible for  
302 gasification during the steam reforming and to oxygen during its combustion activated  
303 by these Ni particles; ii) the shoulder around 500 °C oxidation temperature may be  
304 related to a polymerized coke (graphitic and aromatic) with a more condensate structure  
305 due to self condensation reactions of each compound. This coke is generally less  
306 reactive and progressively separates from Ni sites, thus requiring higher temperatures  
307 for its combustion (above 450 °C), and; iii) between 500 and 700 °C oxidation  
308 temperature, associated with the filamentous coke, which is not adsorbed on Ni sites  
309 and is combusted above 500 °C. This coke grows towards the outside of the catalyst  
310 particles without significantly contributing to catalyst deactivation. From Figure 4 it can  
311 be concluded that the type of model compound significantly affects the nature of the  
312 coke deposited on the catalyst. Thus, the coke derived from oxygenated steam  
313 reforming presented the most heterogeneous structure, with the coke from furfural being  
314 the most filamentous and that derived from phenol and anisole more polymerized. On  
315 the contrary, the coke derived from aromatic hydrocarbons was less developed with a  
316 lower number of shoulders detected in the TPO analysis.

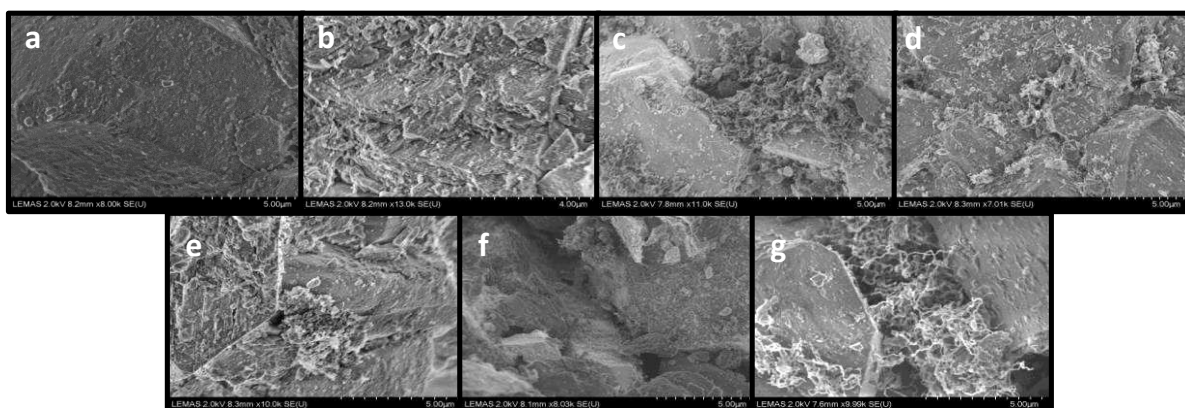


317

318

**Figure 4**

319 Figure 5 shows SEM images of the fresh (a) and the used catalyst in the steam  
 320 reforming of toluene (b), phenol (c), methyl naphthalene (d), indene (e), anisole (f) and  
 321 furfural (g) after reaction. As observed, the SEM analysis confirmed that furfural leads  
 322 to highly developed filamentous type carbon deposits on the catalyst surface. Besides,  
 323 some filamentous coke is observed on the catalyst used in phenol steam reforming, but  
 324 this coke seems to be less structured than that derived from furfural. The steam  
 325 reforming of aromatic hydrocarbons led to mainly non-structured carbon deposits,  
 326 similar to those reported by Josuinkas et al. [28] for toluene/naphthalene steam  
 327 reforming on Ni catalysts prepared from hydrotalcite-like precursors.



328

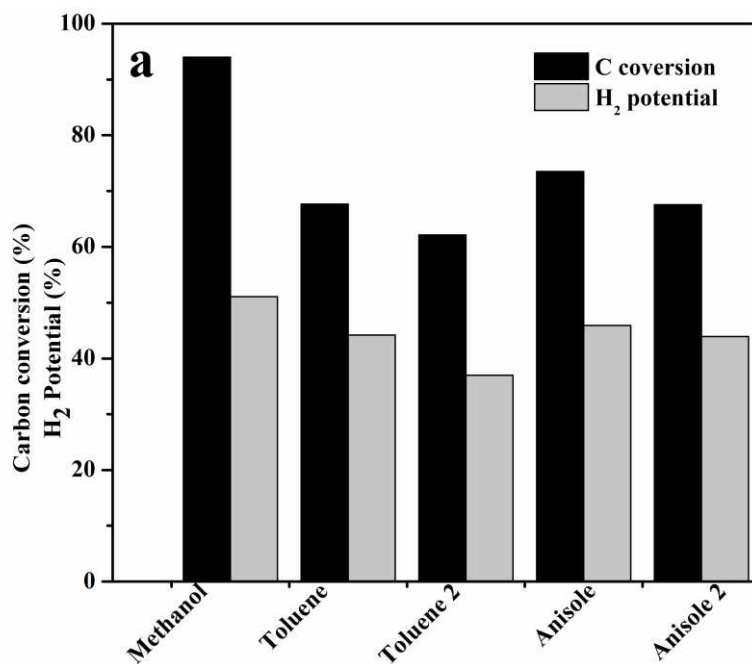
## Figure 5

329

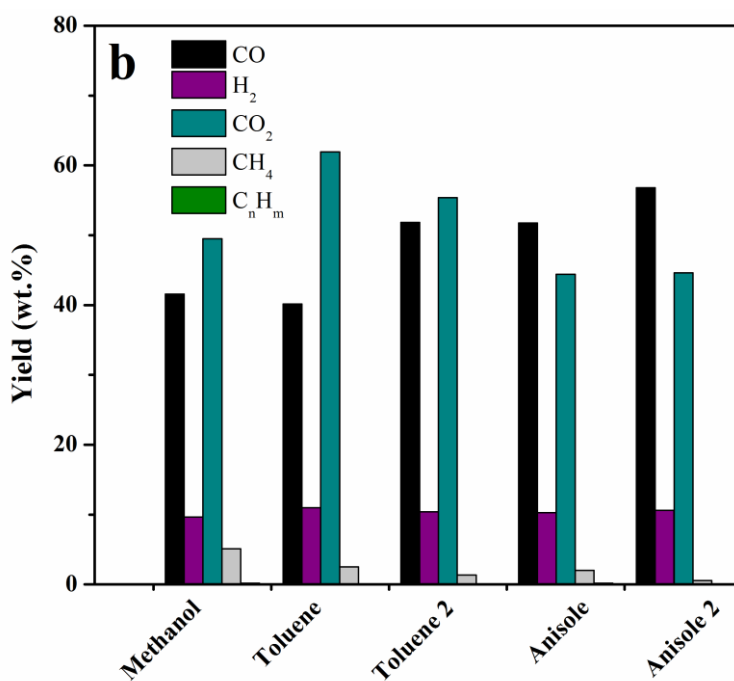
### 330 3.2. Effect of $C_{cc}/C_s$ ratio on the feedstock

331 Figure 6(a) shows the conversion and  $H_2$  potential and (b) shows the gaseous compound  
332 yields in the steam reforming experiments performed with toluene/methanol and  
333 anisole/methanol mixtures with a  $C_{cc}/C_s$  ratio of 2. Furthermore, Figure 6 also  
334 compares these results with those obtained with a  $C_{cc}/C_s$  ratio of 1. In this figure, the  
335 terms anisole1 and toluene 1 correspond to  $C_{cc}/C_s=1$ , whereas anisole 2 and toluene2  
336 correspond to  $C_{cc}/C_s=2$ . As observed in Figure 6(a), when the content of toluene or  
337 anisole increases in the reaction medium, carbon conversion decreases from 67 to 62 wt.  
338 % and from 73 to 67 wt. %, respectively. Likewise,  $H_2$  potential also decreases by  
339 increasing the  $C_{cc}/C_s$  ratio, with this trend being more pronounced in the steam  
340 reforming of toluene (from 44 to 37 %). Therefore, by increasing the concentration of  
341 tar-like compounds in the feedstock and decreasing that of methanol (which is more  
342 reactive and more easily reformed), the steam reforming activity of the mixtures to CO,  
343  $CO_2$  and  $H_2$  is moderately reduced.

344 A low content of methanol also changes the composition of the gas, as observed in  
345 Figure 6(b). When the content of toluene is increased in the feedstock, formation of CO  
346 is favoured (from 40 to 51 %) and that of  $CO_2$  is reduced (from 62 to 55 %). When  
347 anisole content is increased, a similar increasing trend is observed for CO yield (from  
348 52 % to 57 %). However, the yield of  $CO_2$  remained almost constant in the gaseous  
349 stream (around 44 %). It is noteworthy that, in both cases, the yields of  $H_2$  remained  
350 almost constant and those of  $CH_4$  were moderately reduced. These results suggest that  
351 an increase in  $C_{cc}/C_s$  ratio in the feedstock leads to a reduction in the catalyst activity,  
352 especially for WGS reaction, given that higher coke depositions reduce catalyst activity  
353 for this reaction.



354



355

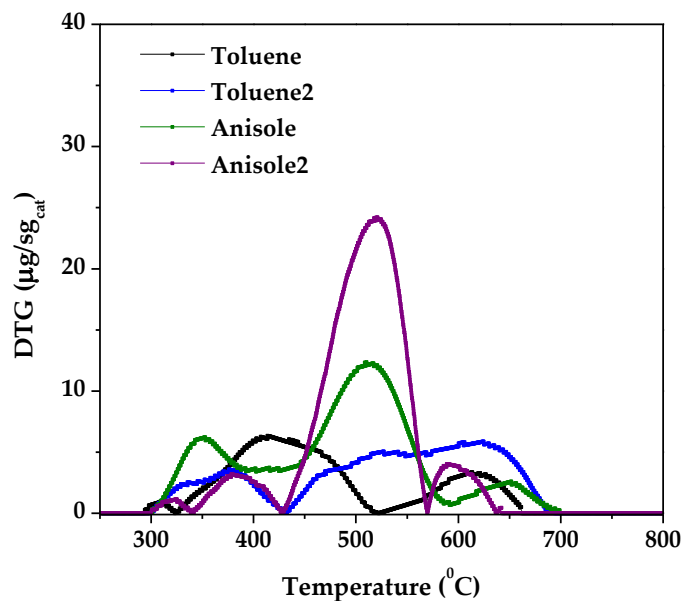
356

**Figure 6**

357 The steam reforming literature contains mainly global data for different catalysts on the  
 358 conversion of tar model compounds, but very few reports deal with the influence of  
 359 their concentration in the feedstock. Thus, only Ma et al. [36] established that higher

360 loadings of benzene or naphthalene in the biomass gasification derived tar resulted in a  
361 reduction of their conversion in a catalytic tar removal system.

362 DTG-TPO results for the Ni/Al<sub>2</sub>O<sub>3</sub> catalyst used in the catalytic reforming of toluene  
363 and anisole with a C<sub>cc</sub>/ C<sub>s</sub> ratio of 2 (Figure 7) showed an increase in the coke amount  
364 formed compared to the results obtained with a C<sub>cc</sub>/ C<sub>s</sub> ratio of 1, i.e., from 0.81 % to  
365 1.4% in the reforming of toluene and from 1.49 % to 2.75 % in the reforming of  
366 anisole. Although the deactivation of the catalyst is not significant, a higher  
367 concentration of the model compound in the feedstock implies a lower conversion along  
368 with an increase in CO selectivity, thus promoting carbon deposition by CO  
369 disproportionation [31]. Moreover, the nature of the coke deposited on the catalyst  
370 changes depending on the reactant loading. The catalyst used for toluene with a C<sub>cc</sub>/ C<sub>s</sub>  
371 ratio of 2 presents a higher shoulder at low temperatures (400 °C) and a lower peak at  
372 higher temperatures (500-600 °C), whereas this peak is considerably higher when the  
373 C<sub>cc</sub>/ C<sub>s</sub> ratio of anisole increases from 1 to 2 in the feedstock. Thus, Figure 7 suggests  
374 that an increase in the content of toluene results in an increase in the amorphous coke  
375 (which can be more easily removed), whereas a higher amount of anisole leads to the  
376 formation of a more condensed and structured coke (with higher degree of  
377 graphitization).



378

379

**Figure 7**

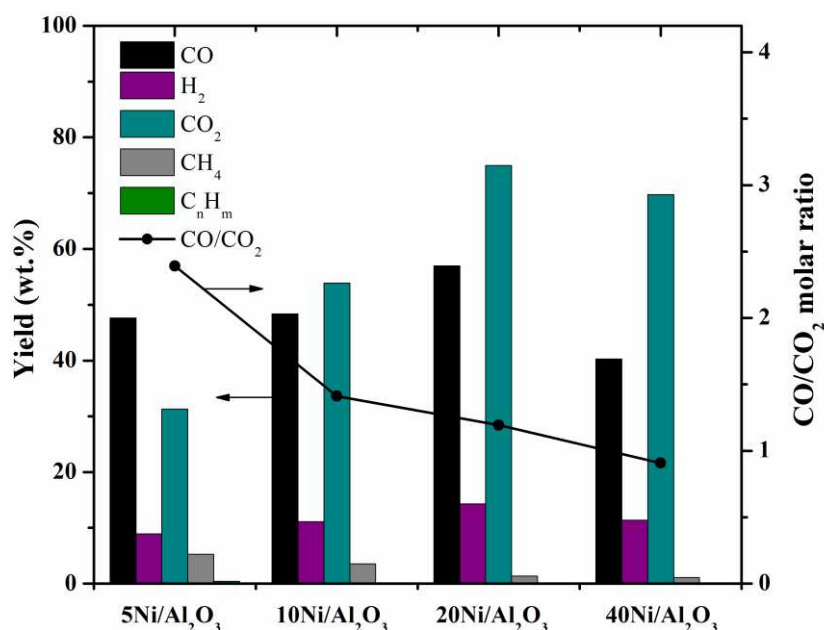
380 3.3. Effect of Ni loading on the catalyst

381 The influence of Ni content on the reforming performance of a mixture of all the model  
 382 compounds previously studied separately (maintaining a  $C_s/C_{cc}$  ratio of 1) is discussed  
 383 in this section. The sample notation indicates the amount of Ni deposited on the support,  
 384 for example, 5Ni/Al<sub>2</sub>O<sub>3</sub> means that the catalyst contains 5 wt.% Ni. Figure 8 shows the  
 385 carbon conversion and H<sub>2</sub> potential obtained at 750 °C and for a reaction time of 60 min  
 386 using the Ni/Al<sub>2</sub>O<sub>3</sub> catalyst with different Ni loadings. As observed, the conversion of  
 387 the mixture increases from 65 to 90 % when Ni loading is increased from 5 to 20 wt.%.  
 388 As Ni content is further increased to 40 wt.%, the conversion of the mixture decreases  
 389 to 73 %. The same trend was observed for the H<sub>2</sub> potential, attaining its maximum value  
 390 (63 %) with 20Ni/Al<sub>2</sub>O<sub>3</sub> catalyst. Thus, by increasing Ni content to 20 wt.%, more  
 391 active sites will be available for the reforming and WGS reactions, which would result  
 392 in higher carbon conversions and H<sub>2</sub> yields [37]. However, higher Ni contents in the  
 393 catalyst may contribute to higher coke formation, thereby deactivating faster  
 394 40Ni/Al<sub>2</sub>O<sub>3</sub> catalyst, and consequently lowering tar conversion for 60 min reaction.

395 According to Li et al. [39], an increase in Ni loading promotes the activity of the  
396 catalyst, but cannot prevent the deactivation in the acetic acid steam reforming. These  
397 authors observed that nickel species probably aggregate in the catalyst preparation  
398 process when Ni loadings are higher than 20 %, thus forming large size particles (with a  
399 significant presence of crystallites), and therefore leading to faster metal sintering and  
400 coke deposition on the catalyst. Similarly, Yue et al. [39] and Josuinkas et al. [28]  
401 suggested that a decrease in tar conversion for high Ni contents is associated with an  
402 increase in Ni particle size and the consequent decrease in the catalyst surface area and  
403 activity.

#### 404 **Figure 8**

405 Figure 9 shows the gaseous product yields and CO/CO<sub>2</sub> molar ratios obtained in the  
406 steam reforming of the mixture with different Ni loadings. The CO, CO<sub>2</sub> and H<sub>2</sub> yields  
407 by mass unit in the feed increase as Ni content is increased to 20 wt.% due to the  
408 enhancement of steam reforming and WGS reactions as well as decomposition reactions  
409 [39]. However, a further increase in Ni content above 20 wt.% leads to a decrease of  
410 their yields, given that the total conversion of the feed is reduced, as was previously  
411 reported (Figure 8). In addition, Figure 9 shows that CO/CO<sub>2</sub> molar ratio decreases by  
412 increasing Ni content, even for 40Ni/Al<sub>2</sub>O<sub>3</sub> catalyst, indicating that the WGS reaction is  
413 more favoured [40]. It should be noted that the drop of CO/CO<sub>2</sub> ratio, especially when  
414 Ni content increases from 20 to 40 %, may also be attributed to the Boudouard reaction  
415 occurring when the catalyst undergoes a severe coke deposition. Furthermore, when Ni  
416 content in the catalyst was 20 wt.% and 40 wt.%, the yields of CH<sub>4</sub> were almost  
417 negligible (1.3 and 1.0 wt. %, respectively). These results suggest that 20Ni/Al<sub>2</sub>O<sub>3</sub>  
418 catalyst is the most suitable for reforming the tars derived from biomass gasification.



419

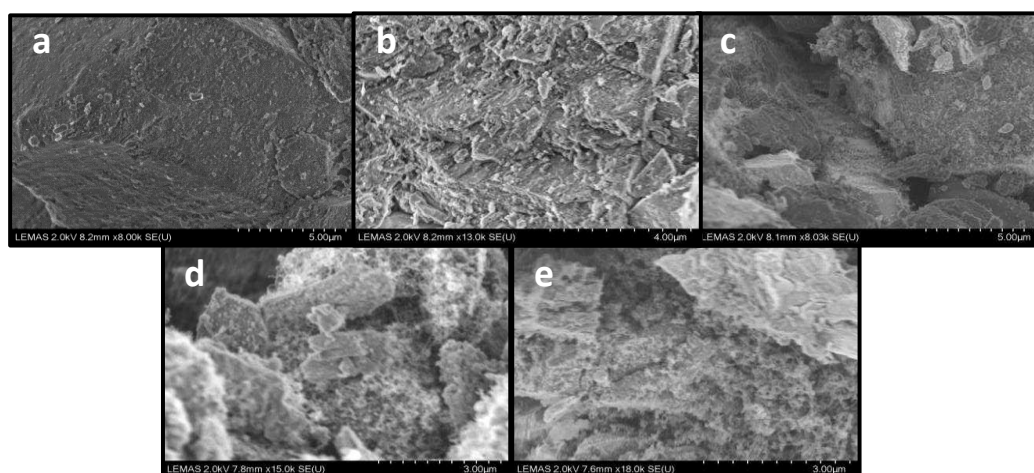
420

**Figure 9**

421 Other papers in the literature also report an optimum Ni content in the catalyst for tar  
 422 conversion to H<sub>2</sub> and CO. Seyedeyn-Azad et al. [40] found that the highest catalytic  
 423 activity for the steam reforming of biomass derived bio-oil, both in terms of hydrogen  
 424 production and selectivity, was for a Ni/Al<sub>2</sub>O<sub>3</sub> catalyst with a Ni content of 14.1 %. For  
 425 higher Ni loadings (18 %), the results did not change significantly. Yue et al. [39]  
 426 performed the steam reforming of toluene on NiO/MgO-γAl<sub>2</sub>O<sub>3</sub> and observed 100%  
 427 conversion when Ni content was 10 %, but an increase to 15 % led to conversion  
 428 decrease to 86 %. Similarly, Wang et al. [37] obtained the highest conversion and H<sub>2</sub>  
 429 yield in the steam reforming of acetic acid and hydroxyacetone with a Ni/nano- Al<sub>2</sub>O<sub>3</sub>  
 430 catalyst loaded with 10 % Ni. Nevertheless, other works concluded that the catalytic  
 431 activity in the reforming reactions increased with higher Ni contents. For example,  
 432 Garbarino et al. [33] determined that the conversion of a phenol-ethanol mixture on Ni  
 433 supported catalysts was as follows: Ni39>Ni16>Ni5.

434 The amounts of coke deposited on 5, 10, 20 and 40 Ni/Al<sub>2</sub>O<sub>3</sub> catalysts, considering that  
435 total weight loss during TPO analysis corresponds to carbon oxidation, are 0.6, 0.85, 2.2  
436 and 6.5 wt. %, respectively. Carbon deposition increases by increasing Ni content and,  
437 although the 40Ni/Al<sub>2</sub>O<sub>3</sub> catalyst still promotes the steam reforming activity, it cannot  
438 prevent the higher coke formation rates. As shown in Figure 9, Ni loading significantly  
439 affects the distribution of reforming products, which will further affect coke formation,  
440 since some compounds, such as CO, will be potential coke precursors. Furthermore, it  
441 seems that a bigger Ni particle size in 40Ni/Al<sub>2</sub>O<sub>3</sub> catalyst would favour CO  
442 disproportionation, thus leading to a higher catalyst deactivation [38].

443 Figure 10 shows in detail the morphology of the carbon species in the fresh (a) and used  
444 catalysts containing 5 (b), 10 (c), 20 (d) and 40 (e) wt.% Ni. As observed, the SEM  
445 analysis confirmed the presence of filamentous type carbon deposits on the catalysts  
446 surface, with the amount of deposited coke being higher as Ni loading is increased.  
447 These results are consistent with those obtained in the TPO, in which the highest coke  
448 yields have been obtained with 40Ni/Al<sub>2</sub>O<sub>3</sub> catalyst.



449

450

**Figure 10**

451 **4. Conclusions**

452 Steam reforming of different aromatic and oxygenated tar model compounds and their  
453 mixture has been studied on Ni/Al<sub>2</sub>O<sub>3</sub> catalysts. The highest conversions and H<sub>2</sub>  
454 potentials were obtained for oxygenated compounds, and specifically for anisole,  
455 whereas methylnaphthalene presented the lowest reactivity. Although carbon deposition  
456 on the catalyst was low in all the experiments, the amount of coke was higher with  
457 oxygenate reactants due to their higher reactivity favouring unwanted reactions that  
458 promoted its formation. Increasing the C<sub>cc</sub>/ C<sub>s</sub> ratio to 2, the steam reforming activity to  
459 CO, CO<sub>2</sub> and H<sub>2</sub> was slightly lower for toluene than anisole and the coke deposited on  
460 the catalyst increased due the higher CO selectivity. Besides, the nature of the coke was  
461 disparate using toluene and anisole, increasing the amorphous coke with the former and  
462 the graphitization degree with the latter. Moreover, Ni loading increase enhances  
463 reforming and WGS reactions, thereby increasing carbon conversion and H<sub>2</sub> potential.  
464 However, for a Ni loading of 40 %, conversion decreases due the reduction in the  
465 catalyst specific surface area, which can be associated with an increase in Ni particle  
466 size. Besides, higher Ni loading lead to higher amount of coke with a more developed  
467 filamentous structure.

#### 468 **Acknowledgments**

469 Maite Artetxe and Jon Alvarez thank the University of the Basque Country UPV/EHU  
470 for their post-graduate Grant (UPV/EHU 2013 and 2015, respectively). We also  
471 acknowledge support from the UK Engineering & Physical Sciences Research Council  
472 through Supergen Bioenergy Grant EP/M013162/1.

473

474

475 **Reference List**

- 476 [1] S. Heidenreich, P.U. Foscolo, New concepts in biomass gasification, *Prog. Energy*  
477 *Combust. Sci.* 46 (2015) 72-95.
- 478 [2] C. Font Palma, Modelling of tar formation and evolution for biomass gasification: A  
479 review, *Appl. Energy* 111 (2013) 129-141.
- 480 [3] R. Coll, J. Salvadó, X. Farriol, D. Montané, Steam reforming model compounds of  
481 biomass gasification tars: conversion at different operating conditions and tendency  
482 towards coke formation, *Fuel Process. Technol.* 74 (2001) 19-31.
- 483 [4] S. Anis, Z.A. Zainal, Tar reduction in biomass producer gas via mechanical,  
484 catalytic and thermal methods: A review, *Renew. Sustain. Energy Rev.* 15 (2011) 2355-  
485 2377.
- 486 [5] G. Guan, M. Kaewpanha, X. Hao, A. Abudula, Catalytic steam reforming of  
487 biomass tar: Prospects and challenges, *Renew. Sustain. Energy Rev.* 58 (2016) 450-461.
- 488 [6] Y. Shen, K. Yoshikawa, Recent progresses in catalytic tar elimination during  
489 biomass gasification or pyrolysis—A review, *Renew. Sustain. Energy Rev.* 21 (2013)  
490 371-392.
- 491 [7] J. Ashok, Y. Kathiraser, M.L. Ang, S. Kawi, Bi-functional hydrotalcite-derived  
492 NiO–CaO–Al<sub>2</sub>O<sub>3</sub> catalysts for steam reforming of biomass and/or tar model compound  
493 at low steam-to-carbon conditions, *Appl. Catal. B.* 172–173 (2015) 116-128.
- 494 [8] S. Sayas, A. Chica, Furfural steam reforming over Ni-based catalysts. Influence of  
495 Ni incorporation method, *Int. J. Hydrogen Energy* 39 (2014) 5234-5241.
- 496 [9] M. Koike, D. Li, H. Watanabe, Y. Nakagawa, K. Tomishige, Comparative study on  
497 steam reforming of model aromatic compounds of biomass tar over Ni and Ni–Fe alloy  
498 nanoparticles, *Appl. Catal. A.* 506 (2015) 151-162.
- 499 [10] D. Yao, C. Wu, H. Yang, Q. Hu, M.A. Nahil, H. Chen, P.T. Williams, Hydrogen  
500 production from catalytic reforming of the aqueous fraction of pyrolysis bio-oil with  
501 modified Ni–Al catalysts, *Int. J. Hydrogen Energy* 39 (2014) 14642-14652.
- 502 [11] C. Montero, A. Ochoa, P. Castaño, J. Bilbao, A.G. Gayubo, Monitoring NiO and  
503 coke evolution during the deactivation of a Ni/La<sub>2</sub>O<sub>3</sub>– $\alpha$ -Al<sub>2</sub>O<sub>3</sub> catalyst in ethanol steam  
504 reforming in a fluidized bed, *J. Catal.* 331 (2015) 181-192.
- 505 [12] S. Chitsazan, S. Sepehri, G. Garbarino, M.M. Carnasciali, G. Busca, Steam  
506 reforming of biomass-derived organics: Interactions of different mixture components on  
507 Ni/Al<sub>2</sub>O<sub>3</sub> based catalysts, *Appl. Catal. B.* 187 (2016) 386-398.
- 508 [13] R. Michel, A. Łamacz, A. Krzton, G. Djéga-Mariadassou, P. Burg, C. Courson, R.  
509 Gruber, Steam reforming of  $\alpha$ -methylnaphthalene as a model tar compound over olivine  
510 and olivine supported nickel, *Fuel* 109 (2013) 653-660.

- 511 [14] C. Wu, P.T. Williams, Hydrogen production by steam gasification of  
512 polypropylene with various nickel catalysts, *Appl. Catal. B* 87 (2009) 152-161.
- 513 [15] J. Alvarez, S. Kumagai, C. Wu, T. Yoshioka, J. Bilbao, M. Olazar, P.T. Williams,  
514 Hydrogen production from biomass and plastic mixtures by pyrolysis-gasification, *Int.*  
515 *J. Hydrogen Energy* 39 (2014) 10883-10891.
- 516 [16] B. Valle, A. Remiro, A.T. Aguayo, J. Bilbao, A.G. Gayubo, Catalysts of Ni/ $\alpha$ -  
517 Al<sub>2</sub>O<sub>3</sub> and Ni/La<sub>2</sub>O<sub>3</sub>- $\alpha$ -Al<sub>2</sub>O<sub>3</sub> for hydrogen production by steam reforming of bio-oil  
518 aqueous fraction with pyrolytic lignin retention, *Int. J. Hydrogen Energy* 38 (2013)  
519 1307-1318.
- 520 [17] S. Wang, X. Li, F. Zhang, Q. Cai, Y. Wang, Z. Luo, Bio-oil catalytic reforming  
521 without steam addition: Application to hydrogen production and studies on its  
522 mechanism, *Int. J. Hydrogen Energy* 38 (2013) 16038-16047.
- 523 [18] M. Artetxe, M.A. Nahil, M. Olazar, P.T. Williams, Steam reforming of phenol as  
524 biomass tar model compound over Ni/Al<sub>2</sub>O<sub>3</sub> catalyst, *Fuel* 184 (2016) 629-636.
- 525 [19] D. Li, M. Tamura, Y. Nakagawa, K. Tomishige, Metal catalysts for steam  
526 reforming of tar derived from the gasification of lignocellulosic biomass, *Bioresour.*  
527 *Technol.* 178 (2015) 53-64.
- 528 [20] C. Pfeifer, H. Hofbauer, Development of catalytic tar decomposition downstream  
529 from a dual fluidized bed biomass steam gasifier, *Powder Technol.* 180 (2008) 9-16.
- 530 [21] A. Arregi, G. Lopez, M. Amutio, I. Barbarias, J. Bilbao, M. Olazar, Hydrogen  
531 production from biomass by continuous fast pyrolysis and in-line steam reforming, *RSC*  
532 *Adv.* (2016) 25975-25985.
- 533 [22] D. Li, C. Ishikawa, M. Koike, L. Wang, Y. Nakagawa, K. Tomishige, Production  
534 of renewable hydrogen by steam reforming of tar from biomass pyrolysis over  
535 supported Co catalysts, *Int. J. Hydrogen Energy* 38 (2013) 3572-3581.
- 536 [23] R. Zhang, Y. Wang, R.C. Brown, Steam reforming of tar compounds over  
537 Ni/olivine catalysts doped with CeO<sub>2</sub>, *Energy Convers. Manage.* 48 (2007) 68-77.
- 538 [24] C. Parsland, A. Larsson, P. Benito, G. Fornasari, J. Brandin, Nickel-substituted  
539 bariumhexaaluminates as novel catalysts in steam reforming of tars, *Fuel Process.*  
540 *Technol.* 140 (2015) 1-11.
- 541 [25] R. González-Gil, I. Chamorro-Burgos, C. Herrera, M.A. Larrubia, M. Laborde, F.  
542 Mariño, L.J. Alemany, Production of hydrogen by catalytic steam reforming of  
543 oxygenated model compounds on Ni-modified supported catalysts. Simulation and  
544 experimental study, *Int. J. Hydrogen Energy* 40 (2015) 11217-11227.
- 545 [26] A. Lamacz, A. Krztoń, G. Djéga-Mariadassou, Steam reforming of model  
546 gasification tars compounds on nickel based ceria-zirconia catalysts, *Catal. Today* 176  
547 (2011) 347-351.

- 548 [27] R. Trane-Restrup, A.D. Jensen, Steam reforming of cyclic model compounds of  
549 bio-oil over Ni-based catalysts: Product distribution and carbon formation, *Appl. Catal.*  
550 *B.165* (2015) 117-127.
- 551 [28] F.M. Josuinkas, C.P.B. Quitete, N.F.P. Ribeiro, M.M.V.M. Souza, Steam  
552 reforming of model gasification tar compounds over nickel catalysts prepared from  
553 hydrotalcite precursors, *Fuel Process Technol* 121 (2014) 76-82.
- 554 [29] S. Czernik, R. Evans, R. French, Hydrogen from biomass-production by steam  
555 reforming of biomass pyrolysis oil, *Catal. Today* 129 (2007) 265-268.
- 556 [30] D. Wang, D. Montané, E. Chornet, Catalytic steam reforming of biomass-derived  
557 oxygenates: acetic acid and hydroxyacetaldehyde, *Appl. Catal. A.143* (1996) 245-270.
- 558 [31] X. Hu, G. Lu, Investigation of the steam reforming of a series of model compounds  
559 derived from bio-oil for hydrogen production, *Appl. Catal. B.88* (2009) 376-385.
- 560 [32] R.R. Davda, J.W. Shabaker, G.W. Huber, R.D. Cortright, J.A. Dumesic, A review  
561 of catalytic issues and process conditions for renewable hydrogen and alkanes by  
562 aqueous-phase reforming of oxygenated hydrocarbons over supported metal catalysts,  
563 *Appl. Catal. B.56* (2005) 171-186.
- 564 [33] G. Garbarino, A. Lagazzo, P. Riani, G. Busca, Steam reforming of ethanol-phenol  
565 mixture on Ni/Al<sub>2</sub>O<sub>3</sub>: Effect of Ni loading and sulphur deactivation, *Appl. Catal. B.129*  
566 (2013) 460-472.
- 567 [34] J. Remón, F. Broust, G. Volle, L. García, J. Arauzo, Hydrogen production from  
568 pine and poplar bio-oils by catalytic steam reforming. Influence of the bio-oil  
569 composition on the process, *Int. J. Hydrogen Energy* 40 (2015) 5593-5608.
- 570 [35] A. Remiro, B. Valle, A.T. Aguayo, J. Bilbao, A.G. Gayubo, Operating conditions  
571 for attenuating Ni/La<sub>2</sub>O<sub>3</sub>- $\alpha$ -Al<sub>2</sub>O<sub>3</sub> catalyst deactivation in the steam reforming of bio-  
572 oil aqueous fraction, *Fuel Process. Technol.* 115 (2013) 222-232.
- 573 [36] L. Ma, H. Verelst, G.V. Baron, Integrated high temperature gas cleaning: Tar  
574 removal in biomass gasification with a catalytic filter, *Catal. Today* 105 (2005) 729-  
575 734.
- 576 [37] S. Wang, Q. Cai, F. Zhang, X. Li, L. Zhang, Z. Luo, Hydrogen production via  
577 catalytic reforming of the bio-oil model compounds: Acetic acid, phenol and  
578 hydroxyacetone, . *J. Hydrogen Energy* 39 (2014) 18675-18687.
- 579 [38] Z. Li, X. Hu, L. Zhang, S. Liu, G. Lu, Steam reforming of acetic acid over Ni/ZrO<sub>2</sub>  
580 catalysts: Effects of nickel loading and particle size on product distribution and coke  
581 formation, *Appl. Catal. A.417-418* (2012) 281-289.
- 582 [39] B. Yue, X. Wang, X. Ai, J. Yang, L. Li, X. Lu, W. Ding, Catalytic reforming of  
583 model tar compounds from hot coke oven gas with low steam/carbon ratio over  
584 Ni/MgO-Al<sub>2</sub>O<sub>3</sub> catalysts, *Fuel Process Technol* 91 (2010) 1098-1104.

585 [40] F. Seyedejn-Azad, E. Salehi, J. Abedi, T. Harding, Biomass to hydrogen via  
586 catalytic steam reforming of bio-oil over Ni-supported alumina catalysts, Fuel .Process  
587 Technol. 92 (2011) 563-569.

588

589

590 **Figure captions**

591 Figure 1. Schematic diagram of the experimental system.

592 Figure 2. Carbon conversion and H<sub>2</sub> potential in the steam reforming of different tar  
593 model compounds.

594 Figure 3. Gaseous compound yields in the steam reforming of different tar model  
595 compounds.

596 Figure 4. DTG-TPO curves of the coke deposited on the catalyst used with each tar  
597 model compounds.

598 Figure 5. SEM imagines of the fresh (a) and the used catalyst used with toluene (b),  
599 phenol (c), methyl naphthalene (d), indene (e), anisole (f) and furfural (g).

600 Figure 6. Effect of C<sub>cc</sub>/ C<sub>s</sub> ratio on carbon conversion and H<sub>2</sub> potential (a) and on gas  
601 compounds yields (b) in the steam reforming of toluene and anisole.

602 Figure 7. DTG-TPO curves of the coke deposited on the catalyst used with different  
603 C<sub>cc</sub>/ C<sub>s</sub> ratios in the feedstock of toluene and anisole.

604 Figure 8. Effect of Ni content in the catalyst on carbon conversion and H<sub>2</sub> potential of  
605 a mixture of all the model compounds.

606 Figure 9. Effect of Ni content in the catalyst on gaseous compound yields and  
607 CO/CO<sub>2</sub> molar ratio of a mixture of all the model compounds.

608 Figure 10. SEM imagines of the fresh (a) and used catalysts used with Ni contents of 5  
609 (b), 10 (c), 20 (d) and 40 (e).

610